

Introduction

Measurement of tool wear is extraordinarily necessary to predict the helpful lifetime of tool inserts. is can be useful to watch and to

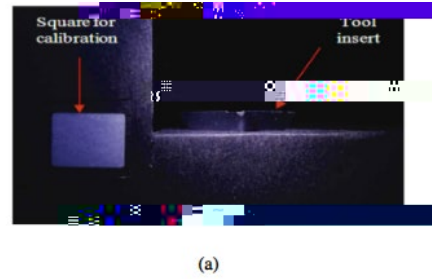


Figure 1: Schematic diagram of the tool wear measurement system.

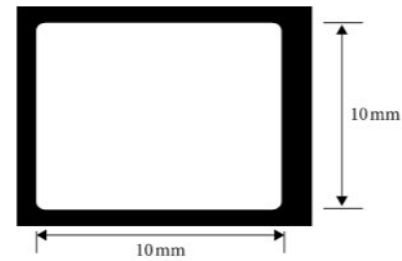
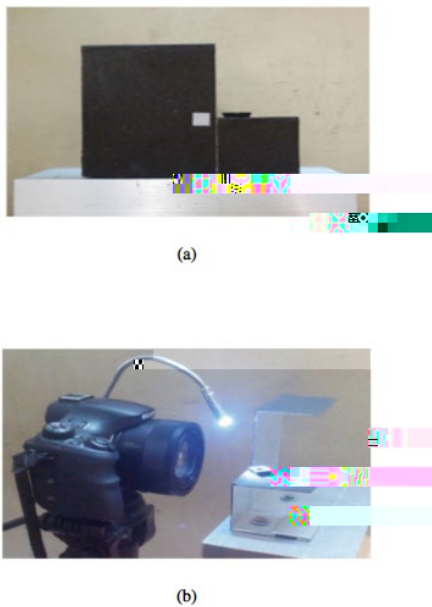


Figure 3: (a) Captured image of the worn out insert; (b) processed image of the calibration square.

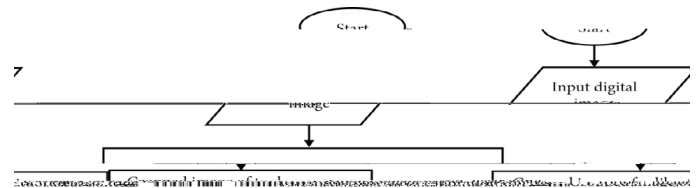


Figure 4: Flowchart of the algorithm for image processing.

of tool insert and standardization sq. The fixture has been developed for correct positioning of tool insert and therefore the standardization sq. (Figure 2a) shows the designed fixture for this purpose [7]. The standardization sq. was fixed on a vertical plate of fixture. The fixture was lined with a black paper to avoid the reflection of sunshine. This sq. is additionally used for outlining the origin of the virtual system developed for the mensuration of tool wear volume. The vertical plate has provision to maneuver forward and backward in order that the plane of standardization sq. and tip of tool insert remains same. The position of the camera, source of illumination, fixture, and insert is indicated in (Figure 2b). The image has been captured specified it contains each the standardization sq. and gear insert as indicated in (Figure 3a). (Figure 3b) shows the processed image of the standardization sq. [8]. (Figure 4) shows a flow diagram of associate rule for image process to calculate tool wear parameters (Figure 5) indicates the results of various stages of the image processing algorithm. (Figure 5a) indicates the grayscale image of the tool wear zone. (Figure 5b) indicates the binary image of the segmented tool wear zone obtained by using Otsu's thresholding method [9].

Results

In this section, the ultimate results of measurements of 3 tool wear

parameters measured by the vision system are given. For the measuring of the damage of tool insert, the turning experiments area unit conducted on low steel that is wide used for the assembly of bearing cowl of AN IC engine. Turning operations area unit conducted on a CNC turning machine for the machining of internal diameter [10].

The details of the machining parameters area unit indicated in (Table 1). For each turning operation, contemporary inorganic compound insert was employed in that the machining and machining parameters were unbroken same. Machining time needed for each specimen was around five minutes [11]. (Table 2) indicates the small print of machining times for all the inserts. When the machining operation, the tool wear parameters of all the inserts were measured by the vision system [12]. So as to validate the accuracy of the developed

for the measuring of tool wear parameters. With this activity system, there's no would like for separate activity of the vision system. The measurements of a median tool wear dimension with this vision system area unit found to be in shut agreement therewith with the digital magnifier. The common absolute error in mensuration average tool wear dimension for all the twelve inserts was found to be three.08%. Average wear dimension, wear area, and wear perimeter were seen increasing with the machining time. The scanning negatron micrographs indicate severe abrasion marks and harm to the innovative within the case of upper machining time. This study shows that the machine vision system will be effectively wont to live all tool wear parameters and therefore presents the proper and complete image of the tool wear. This system is going to be extraordinarily helpful for producing business to observe tool wear effectively instead of relying just one parameter. This may be extraordinarily helpful to review the results of tool decline quality of machined surface and economy of machining method.

Conflicts of Interest

The authors declare that there are no conflicts of interest regarding the publication of this paper.

References

1. Ames A (1935) Aniseikonia-a factor in the functioning of vision. *Am J Ophthalmol* 18: 1014-1020.
2. Rutstein RP, Corliss DA, Fullard RJ (2000) Comparison of aniseikonia as measured by the aniseikonia inspector and the space eikonometer. *Optom Vis Sci* 83: 836-842.
3. Langenbucher AS (2008) Anisometropia and aniseikonia-unsolved problems of cataract surgery. *Klin Monbl Augenheilkd* 225: 763-769.
4. Okamoto F, Sugiura Y, Okamoto Y (2012) Associations between metamorphopsia and foveal microstructure in patients with epiretinal membrane. *Invest Ophthalmol Vis Sci* 53: 6770-6775.
5. Okamoto F, Sugiura Y, Okamoto Y (2014) Time course of changes in aniseikonia and foveal microstructure after vitrectomy for epiretinal membrane. *Ophthalmol* 121: 2255-2260.
6. Kim JH, Kang SW, Kong MG (2013) Assessment of retinal layers and visual rehabilitation after epiretinal membrane removal. *Graefes Arch Clin Exp Ophthalmol* 251: 1055-1064.
7. Benegas NM, Egbert J, Engel WK (1999) Diplopia secondary to aniseikonia associated with macular disease. *Arch Ophthalmol* 117: 896-899.
8. Enoch JM (1997) Management of aniseikonia after intraocular lens implantation or refractive surgery. *J Refract Surg* 13: 79-82.
9. Okamoto F, Sugiura Y, Okamoto Y (2017) Aniseikonia in various retinal disorders. *Graefes Arch Clin Exp Ophthalmol* 255: 1063-1071.
10. Rutstein RP, Fullard RJ, Wilson JA (2015) Aniseikonia induced by cataract surgery and its effect on binocular vision. *Optom Vis Sci*. 92: 201-207.
11. Hodgetts D (2012) Nonsurgical management of diplopia after retinal surgery. *Am Orthopt J* 62: 38-43.
12. Renne G, Benson J, Charnwood L (1953) The physiological basis of sensory fusion. *Acta Ophthalmol* 34: 1-26.
13. Bradley A, Rabin J, Freeman RD (1983) Nonoptical determinants of aniseikonia. *Invest Ophthalmol Vis Sci*. 24: 507-512.
14. De Wit GC, Muraki CS (2006) Field-dependent aniseikonia associated with an epiretinal membrane a case study. *Ophthalmol* 113: 58-62.